

# In situ characterization of a crack trajectory and shear bands interaction in metallic glasses

B. Bouzakher<sup>b</sup>, T. Benameur<sup>a,\*</sup>, A.R. Yavari<sup>c</sup>, H. Sidhom<sup>b</sup>

<sup>a</sup> LGM-LAB-MA05, ENIM, Université de Monastir, 5019 Monastir, Tunisie

<sup>b</sup> LMMP LAB-STI03, Université de Tunis, ESSTT 1008 Tunis, Tunisie

<sup>c</sup> LTPCM, Domaine Universitaire, BP 75, Saint Martin d'Hères 38402, France

Available online 12 October 2006

## Abstract

In situ SEM observations and atomic force microscopy measurements are carried out to follow changes in front of a mode I stationary crack tip initiated at the edge of thin ribbons of  $\text{Cu}_{60}\text{Zr}_{30}\text{Ti}_{10}$ ,  $\text{Zr}_{65}\text{Ni}_{10}\text{Cu}_{15}\text{Al}_{10}$  and  $\text{Pd}_{42.5}\text{Cu}_{30}\text{Ni}_{7.5}\text{P}_{20}$  metallic glasses and maintained at constant external tensile loads. While the Cu- and Zr-based metallic glasses exhibit a nano-scale shear offset in the vicinity of the crack tip, Pd-based metallic glass showed a few regularly spaced shear bands prior to fracture away from the very near crack-tip region. We have found that the discreteness, the interactions of the shear bands and crack blunting in the three metallic glasses are different. AFM frictional analyses illustrate evidence of flow defects in the vein-like structure morphology of the fractured surfaces.

© 2006 Elsevier B.V. All rights reserved.

**Keywords:** Metallic glasses; Shear bands; Atomic force microscopy (AFM)

## 1. Introduction

The development of bulk metallic glasses BMG with a wide glass forming ability and an impressive range of physical and mechanical properties has prompted new interest in their potential as structural materials [1–3]. However, they are limited by the lack of significant plastic deformation below the glass transition temperature  $T_g$ . Indeed, at ambient temperatures inhomogeneous flow in amorphous alloys tends to be concentrated into very narrow shear bands and brittle failure follows shortly after the onset of yielding [4,5]. Moreover, in bending or uniaxial compression testing the nucleation and propagation of multiple shear bands result in behaviour that is elastic, perfectly plastic [6,7]. The observation of the failure surfaces revealed a vein-like structure for both compressive or tensile stress load, indicating that the glass viscosity within these shear bands has greatly decreased. Despite extensive work reported to elucidate the key factors in the flow process for these glassy alloys: the evolution of shear bands is still the topic of much debate [8–10]. It is claimed that increasing shear band nucleation, propagation and their ability for branching retards the onset of fracture [4]. This

raises the possibility of toughness improvement in amorphous composites, in which a second nanophase may deviate, block and even initiate new shear bands [11–13]. However, details of how shear band propagation affects the stress–strain response, as well as whether slip along a shear band is better modeled as the propagation of discrete displacement increments or as a sliding contact between two rigid surfaces remains unclear. In the present work, we attempt to highlight several findings using in situ SEM and AFM characterization of distributed damage zone around micrometric scale mode I cracks initiated at edge of melt spun ribbons of  $\text{Cu}_{60}\text{Zr}_{30}\text{Ti}_{10}$ ,  $\text{Zr}_{65}\text{Ni}_{10}\text{Cu}_{15}\text{Al}_{10}$  and  $\text{Pd}_{42.5}\text{Cu}_{30}\text{Ni}_{7.5}\text{P}_{20}$  metallic glasses with different inherent ductility. The AFM cross section and lateral surface analyses revealed: firstly, that blunting a crack tip is a function of flow processes associated with shear band motion and discreteness rather than that associated with the work of creating new surface. Secondly, evidence of flow defects are observed in AFM frictional images of the vein morphologies.

## 2. Experimental procedures

The  $\text{Cu}_{60}\text{Zr}_{30}\text{Ti}_{10}$ ,  $\text{Zr}_{65}\text{Ni}_{10}\text{Cu}_{15}\text{Al}_{10}$  and  $\text{Pd}_{42.5}\text{Cu}_{30}\text{Ni}_{7.5}\text{P}_{20}$  (in at.%) alloys were synthesized at the LTPCM-Grenoble, by melting a mixture of highly pure metals, at least 99.99%. The amorphicity of ribbons with thickness of 28–30  $\mu\text{m}$  and width of 0.8–1.5 mm, was examined using X-ray diffraction. Fig. 1 shows the experimental set-up used for applying a gradual tensile elonga-

\* Corresponding author.

E-mail address: T.Benameur@enim.rnu.tn (T. Benameur).

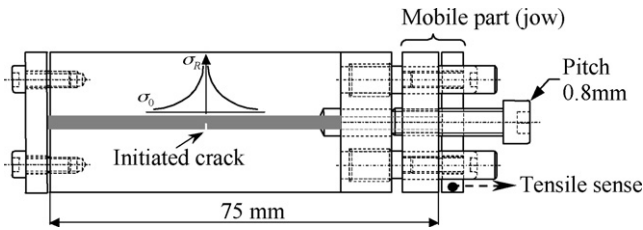


Fig. 1. Experimental set-up: configuration allowing elongation increment of about 0.1 mm.

tion. The ribbons are fixed and submitted to a finite and a gradual displacement steps, each corresponds to an elastic elongation of 0.13%. Before applying the incremental elongation, a mode I micro scaled crack is initiated in the medium region of the ribbon by a pincers. Tensile elongations in the range of 0.13–0.52% have been applied at a strain rate of approximately  $10^{-4} \text{ s}^{-1}$ . The experimental set-up is loaded for each ribbon elongation in the SEM and the AFMs Nanoscope-III Digital microscope chamber for observation of crack behaviour.

**3. Experimental results**

On initial creation of a mode I stationary crack with straight front (with a ratio  $a/w$  of the order of 0.40, where  $a$  and  $w$  are crack’s length and ribbon’s width, respectively), the plastic zone is nearly 80, 70 and 40  $\mu\text{m}$  wide consisting of shear bands running parallel to the crack for  $\text{Cu}_{60}\text{Zr}_{30}\text{Ti}_{10}$ ,  $\text{Zr}_{65}\text{Ni}_{10}\text{Cu}_{15}\text{Al}_{10}$  and  $\text{Pd}_{42.5}\text{Cu}_{30}\text{Ni}_{7.5}\text{P}_{20}$ , respectively, as shown in Fig. 2. The SEM images of the surface located in the vicinity of the crack tip, illustrate the plastic dissipation associated with shear bands formation in  $\text{Cu}_{60}\text{Zr}_{30}\text{Ti}_{10}$  metallic glass as indicated by arrows in Fig. 2a. These shear bands are developed in a large zone

around the crack with a length varying from 40 to 150  $\mu\text{m}$ . The band length seems to be longer in Cu- and Zr-based BMGs compared to that in Pd-based metallic glass (Fig. 2b and c). The AFM topographic analysis of  $\text{Cu}_{60}\text{Zr}_{30}\text{Ti}_{10}$  revealed that shear bands emerged in the vicinity of the crack front and those located far from the crack-tip region have different shear offset and average inter-band distance. Fig. 3a shows a high density of shear bands with an offset varying between 50 and 100 nm. This is in contrast to the shear bands located away from the crack front which are almost regularly spaced (of the order of 1  $\mu\text{m}$ ) and have a large angle with the direction of crack propagation of the order of  $41^\circ$ . The subsidiary shear bands have a lower angle which is found nearly  $11^\circ$ , as indicated by arrow in Fig. 3b. While similar shear band discreteness and subsidiary shear band slides are observed on both Cu- and Zr-based metallic glasses, the  $\text{Pd}_{42.5}\text{Cu}_{30}\text{Ni}_{7.5}\text{P}_{20}$  alloy exhibit only a discrete thin bands, around crack front. A qualitative AFM topographic comparison of the evolution of the crack-tip shape in Pd-, Zr- and Cu-based metallic glasses prior to fracture is shown in Fig. 4a–c. While the crack front of  $\text{Pd}_{42.5}\text{Cu}_{30}\text{Ni}_{7.5}\text{P}_{20}$  is found straight and sharp as seen in Fig. 4a and b illustrating the crack-front of  $\text{Zr}_{65}\text{Cu}_{15}\text{Al}_{10}\text{Ni}_{10}$ , one can distinguish three types of bands. The first type consists of a pilling up of softened shear bands. The second type represents cracked bands. The third type is a set of large area and crack free bands. These morphologies are related to the difference between stress values relative to band localizations. It is interesting to mention that these softened bands have relatively lower frictional property (AFM frictional images not shown). Fig. 4c shows the crack front in  $\text{Cu}_{60}\text{Zr}_{30}\text{Ti}_{10}$ . The front is mainly formed by softened bands and the irregular band shape provides evidence for local adiabatic heating as a result of elastic energy released. The bubble like shapes with different size have the lowest friction magnitude which is an indication of the presence of soft regions in shear bands terraces.

These results are inconsistent with previous high-resolution electron microscopy observations of void-like defects generated in the shear bands resulting from coalescence of excess free volume upon cessation of the plastic flow [14].

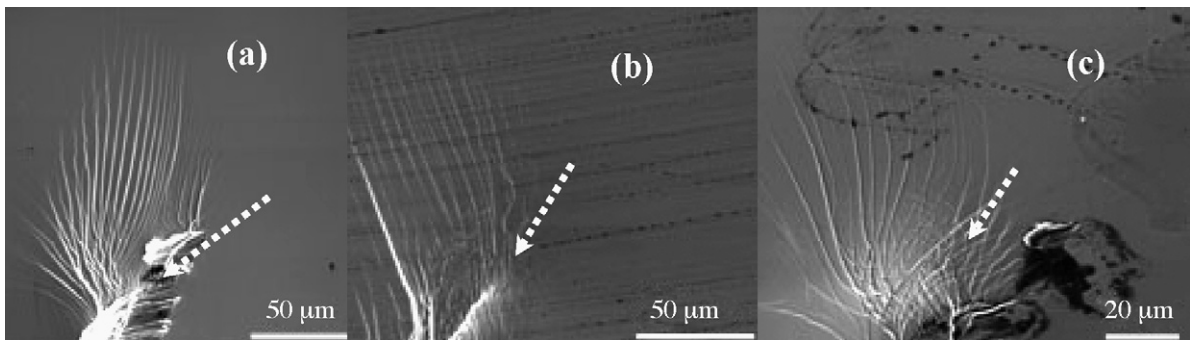


Fig. 2. SEM image of a mode I stationary crack with straight front initiated in ribbons of (a)  $\text{Cu}_{60}\text{Zr}_{30}\text{Ti}_{10}$ , (b)  $\text{Zr}_{65}\text{Ni}_{10}\text{Cu}_{15}\text{Al}_{10}$  and (c)  $\text{Pd}_{42.5}\text{Cu}_{30}\text{Ni}_{7.5}\text{P}_{20}$  metallic glasses.

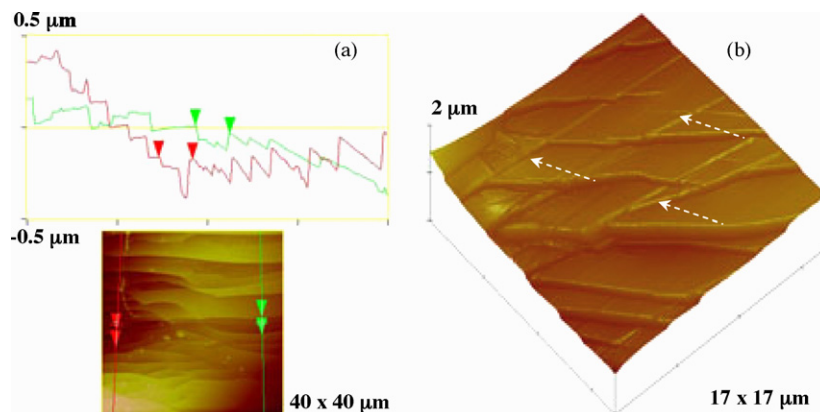


Fig. 3. (a) AFM deflection image and sectional analysis of shear bands discreteness in the vicinity of the crack front. (b) Subsidiary shear bands in  $\text{Cu}_{60}\text{Zr}_{30}\text{Ti}_{10}$  metallic glass.

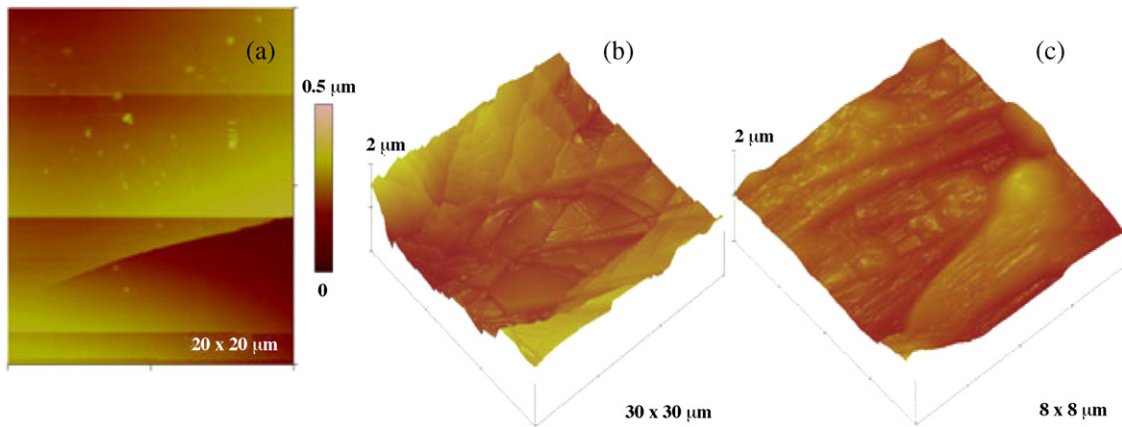


Fig. 4. AFM images of the crack front prior to fracture in (a) Pd<sub>42.5</sub>Cu<sub>30</sub>Ni<sub>7.5</sub>P<sub>20</sub>, (b) Zr<sub>65</sub>Cu<sub>15</sub>Al<sub>10</sub>Ni<sub>10</sub> and (c) a blunted front in Cu<sub>60</sub>Zr<sub>30</sub>Ti<sub>10</sub> metallic glass.

4. Discussion

In conducting in situ AFM topographic and frictional analyses our main concern is with the evolution of discreteness, interaction of shear bands and the change of crack tip’s shape at a blunted mode I crack tip in three metallic glasses with different inherent ductility. In this experimental configuration and prior to unstable crack propagation, irreversible deformation is restricted to the close proximity of the crack tip. In such a case, the direction of crack propagation is perpendicular to the maximum tensile stress in the region of the crack tip. We have found that shear bands evolve differently as function of the magnitude of strain localization and their redirection is sensitive to the stress field distribution. Indeed, Fig. 5a shows the evolution of the inter-band distance IBD as a function of the distance from the crack front type for the three metallic glasses. IBD decreases as strain localization increases, however the large discreteness and subsidiary shear bands observed in Cu- and Zr-based metallic glasses suggest that they are a key factors in the flow process. The distinct plastic dissipation observed in Cu- and Zr-based compared to Pd-based metallic glass may be related to further parameters. In the AFM topographic and frictional analyses a marked change of the crack front prior to fracture in

Cu-based and Zr metallic glasses occurs. Moreover, examination by AFM of the vein-like structure on fracture surfaces of Cu- and Zr-based amorphous alloys is not homogenous but consist of heterogeneous agglomeration of thin and short shear “flow defects” with different qualitative frictional property, as seen in Fig. 5b and c. These results suggest that shear band discreteness, interaction and the amount of elastic energy transformed to local adiabatic heating may play a dual role. On the one hand, the plastic work associated with shear band interaction and discreteness results in effective local adiabatic heating in a blunted crack front, with toughness being much greater than that associated with the work of creating new surface. On the other hand, the local stress concentration associated with discrete, but rigid shear band patterning promotes fracture.

5. Conclusions

In situ SEM and AFM characterization were performed to track the evolution of the crack front, the shear band discreteness and interaction in the vicinity of mode I stationary crack tip initiated at the edge of thin ribbons of monolithic glasses and submitted to constant tensile elongation, the experimental data revealed that:

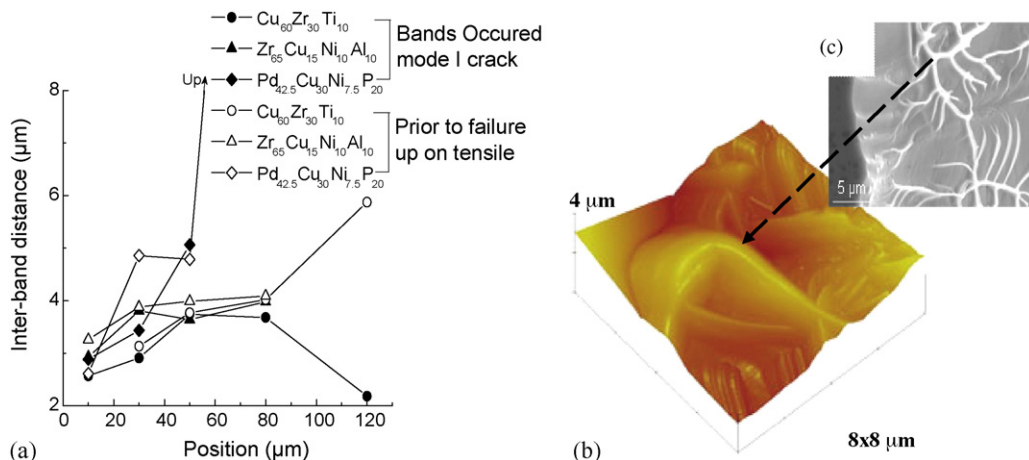


Fig. 5. (a) Inter-shear band average distance as a function of position away from the crack tip for the three metallic glasses (b) SEM image (top) and 8 μm × 8 μm AFM topographic analysis of the vein-like morphology in Cu<sub>60</sub>Zr<sub>30</sub>Ti<sub>10</sub> metallic glass.

- The discreteness and subsidiary shear bands dominate in the vicinity of the crack-tip in Cu- and Zr-based metallic glasses. New formation and branching of certain shear bands were observed. The redirection of shear band is sensitive to the stress field.
- The crack front in  $\text{Cu}_{60}\text{Zr}_{30}\text{Ti}_{10}$ , is mainly formed by softened regions, AFM frictional analysis revealed variation of friction on shear band terrace-like zones which may be due to heterogeneous distribution of free volume. The shear band interaction associated with an effective local adiabatic heating due to partial elastic energy release resulted in a blunted  $\text{Cu}_{60}\text{Zr}_{30}\text{Ti}_{10}$  crack front.
- The vein morphology spreading over the whole fracture surface in Cu- and Zr-based amorphous alloys is not homogenous but formed of agglomeration of flow defects.

### Acknowledgements

This work was supported by the Tunisian ministry of research, technology and competence development. The EU Network entitled “Ductile BMG Composites” MCRTN-CT-

2003-504692 coordinated by A.R. Yavari and technical facilities of INRS/Tunisia are gratefully acknowledged.

### References

- [1] A. Inoue, *Mater. Sci. Found.* 4 (1998) 30–39.
- [2] W.L. Johnson, *Mater. Res. Bull.* 24 (10) (1999) 42–56.
- [3] A. Inoue, *Acta Mater.* 48 (2000) 279.
- [4] T.C. Hufnagel, P. El-Deiry, R.P. Vinci, *Scripta Mater.* 43 (2000) 1071–1076.
- [5] H.A. Bruck, A.J. Rosakis, W.L. Johnson, *J. Mater. Res.* 11 (1996) 503–508.
- [6] C.J. Gilbert, V. Schroeder, R.O. Ritchie, *Metall. Trans. A* 30 (1999) 1739–1754.
- [7] W. Wright, R. Saha, W. Nix, *Mater. Trans. JIM* 42 (2001) 642–649.
- [8] Z. Zhang, J. Eckert, L. Schultz, *Acta Mater.* 51 (2003) 1167–1179.
- [9] K.M. Flores, R.H. Dauskardt, *Intermetallics* 12 (2004) 1025–1029.
- [10] T. Benameur, K. Hajlaoui, G. Heunen, *J. Metastable Nano. Mater.* 17 (2003) 45–54.
- [11] P. Lowhaphandu, J. Lewandowski, *Scripta Mater.* 33 (1998) 1811–1817.
- [12] A. Inoue, W. Zhang, T. Tsurui, A.R. Yavari, A.L. Greer, *Phil. Mag. Lett.* 8 (2005) 221.
- [13] K. Hajlaoui, T. Benameur, G. Vaughan, A.R. Yavari, *Scripta Mater.* 51 (2004) 843–848.
- [14] J. Li, F. Spaepen, T.C. Hufnagel, *Phil. Mag. A* 82 (2002) 2623–2630.